



ELSEVIER

Nuclear Physics A 635 (1998) 231–256

NUCLEAR
PHYSICS A

A Skyrme parametrization from subnuclear to neutron star densities Part II. Nuclei far from stabilities

E. Chabanat^a, P. Bonche^b, P. Haensel^c, J. Meyer^{a,1}, R. Schaeffer^b

^a *Institut de Physique Nucléaire de Lyon, CNRS-IN2P3 / Université Claude Bernard Lyon 1,
43, Bd. du 11.11.18, 69622 Villeurbanne Cedex, France*

^b *Service de Physique Théorique, CEA Saclay, 91191 Gif sur Yvette Cedex, France*

^c *N. Copernicus Astronomical Center, Polish Academy of Sciences, Bartycza 18,
PL-00-716 Warszawa, Poland*

Received 18 July 1997; revised 28 January 1998; accepted 26 March 1998

Abstract

In a first paper Skyrme effective forces were revisited in order to improve their isospin properties away from the β stability line. In this paper, these forces are specifically adjusted to reproduce finite nuclei properties. Spin–orbit terms and center of mass correlations are analyzed. New Skyrme parametrizations are proposed and some of their spectroscopic properties are presented, e.g. S_{2n} , S_{2p} and r.m.s. radii for different isotopic and isotonic series. © 1998 Elsevier Science B.V.

PACS: 21.10.-k; 21.30.+y; 21.60.-n; 21.60.Jz

1. Introduction

In a previous work, hereafter referred as paper I [1], we have presented a *protocol* to characterize Skyrme effective forces to be used both to calculate spectroscopic properties of nuclei and for astrophysical use, such as the neutron star equations of state.

At the beginning of the Skyrme forces history, no information was known concerning the giant monopole resonances and the incompressibility modulus was left as an unknown free parameter. Moreover, because of the limited computational capabilities as compared to now, most calculations were done for rather light nuclei close to sphericity

¹ E-mail jmeyer@ipnl.in2p3.fr.

and in the vicinity of the β -stability line, with the exception of the magic and spherical ^{208}Pb . This lead for instance to the so-called SIII parametrization [2]. The measurement of the giant monopole resonances – breathing modes – gave further constraint on the force and SkM [3] is an example of a Skyrme interaction tailored to account for these resonances. However, large deformations, especially such as those encountered in the description of fission isomers (2 : 1 axis shape ratios) were not correctly reproduced. From SkM, with a slight readjustment of the parameters which was intended to improve the surface tension of SkM, Bartel et al. [4] derived SkM*. This last interaction does account properly for the fission barrier of ^{240}Pu .

This is such a result that in recent years, several Skyrme parametrizations have been used. Let us mention the success of SIII [2] for all spectroscopic properties of nuclei close to sphericity, apart from giant monopole resonances as already mentioned. For substantially deformed systems, forces with an incompressibility modulus around 210 MeV and a more refined surface tension, such as SkM*, are commonly used. Other parametrizations are used for astrophysical properties. Let us recall the work of Tondeur's group – RATP forces [5,6] – releasing some constraints on nuclei but trying to improve upon the equation of state of neutron matter and also upon isospin properties relevant for nucleosynthesis. For very asymmetric matter, Ravenhall et al. [7] have derived an interaction – RBP – which has been successfully used for the equations of state of supernova core during their collapse.

The discovery of super-deformed bands, namely the possibility of a detailed spectroscopic analysis of very deformed systems besides fission isomers, together with the coming availability of radioactive beam facilities and the large number of new exotic nuclei expected to be produced, have lead us in paper I to revisit the *protocol* used to derive all these effective forces. In addition to some small modifications to what had been done for SIII, we decided to implement two ingredients in our *protocol*: i) a value of 230 MeV for the incompressibility modulus of symmetric nuclear matter, ii) a correct reproduction of pure neutron matter, from the recent calculation of Wiringa et al. [8], in order to improve the isospin property of the force away from the β -stability line. Our aim was to obtain a force as good as SIII for nuclei with small deformations, SkM* for large deformations, and which could be used for astrophysical purposes, such as neutron star calculations.

In paper I we have given a detailed discussion of our *protocol*. An application to the equation of state of neutron matter within neutron stars was also presented. Two sets of Skyrme parameters were given which we called SLy230a and SLy230b, the number 230 being to recall the value of the incompressibility modulus to which these forces were adjusted. Starting from SLy230b, we decided to revise slightly our *protocol*, giving more attention to finite nuclei ingredients. Indeed, it seems more reasonable to obtain an effective force valid for very exotic nuclei where many new data are expected, rather than demanding a perfect agreement with pure neutron matter – which remains the result of theoretical estimates, whatever sophisticated they may be. Besides, there are specific terms in the interaction which vanish for infinite matter and are quite relevant for finite nuclei.

In the present study we have derived several new forces according to our *protocol*. To be relevant these forces must be confronted with experimental data and also analyzed with respect to their predictive power. For that purpose we decided to compare their predictions with a *limited set* of experimental data. Indeed our aim is not to provide a full comparison with experiment (see Refs. [9,17] for existing examples where our forces have been already used by different authors in various domains of nuclear structure), rather to select a pertinent benchmark to exemplify the improvement brought by our forces. When no experimental information is known, e.g. toward the drip lines, we have thus decided not to compare the calculation of the isotopic chains we have selected to illustrate our purpose with standard extrapolations [18]. We are quite aware that more extensive calculations are available for other forces, however we think that it is not in the spirit of this work to present similar calculations: the derivation of a new force bringing definite improvements over older ones is already a task in itself.

From the above considerations, this work is organized as follows. After some basic theoretical framework for Skyrme interaction in the next section, we proceed by recalling the *protocol* which was used in our previous work [1]. Then we discuss the modifications introduced specifically for nuclei and present our new set of parameters which we call SLy4. Other sets are discussed – SLy5, SLy6 and SLy7 – arising either from a spin-gradient term usually omitted, or from a more refined two-body center of mass correction, or both. In the fourth section we introduce the force used in the particle-particle channel to account for pairing correlations – a surface delta density dependent one – and we present results for binding energies and radii, isotopic shifts in Pb and some calculations close to the drip lines. As we did not constrain the force on any surface property, we decided to present in Section 5 calculations in the extreme case of the ^{240}Pu fission barrier to check the quality of the obtained forces. In the following two sections, we present first some study of the spin-orbit term, then some preliminary exploration of the nuclear magicity close to the neutron drip line. Finally Section 8 presents our conclusions.

2. Skyrme effective interactions

From the *standard* form we have used in the new Skyrme parametrizations (see Eq. (2.1) in ref [1]), the total binding energy of a nucleus is expressed using a density functional $\mathcal{H}(\mathbf{r})$ which can be split into a sum of terms associated to the different parts of the force:

$$\mathcal{H} = \mathcal{K} + \mathcal{H}_0 + \mathcal{H}_3 + \mathcal{H}_{\text{eff}} + \mathcal{H}_{\text{fin}} + \mathcal{H}_{\text{so}} + \mathcal{H}_{\text{sg}} + \mathcal{H}_{\text{Coul}}, \quad (2.1)$$

where $\mathcal{K} = (\hbar^2/2m)\tau$ is the kinetic energy term, \mathcal{H}_0 a zero range term, \mathcal{H}_3 the density dependent term, \mathcal{H}_{eff} an effective mass term, \mathcal{H}_{fin} a finite range term, \mathcal{H}_{so} a spin-orbit term and \mathcal{H}_{sg} a term due to the tensor coupling with spin and gradient. The exchange part of the coulomb term is calculated with the Slater approximation [19,20] To specify our notations, we recall below some of the relevant expressions already given in paper I:

$$\mathcal{H}_0 = \frac{1}{4}t_0 \left[(2 + x_0) \rho^2 - (2x_0 + 1) (\rho_p^2 + \rho_n^2) \right],$$

$$\begin{aligned}
\mathcal{H}_3 &= \frac{1}{24} t_3 \rho^\alpha \left[(2 + x_3) \rho^2 - (2x_3 + 1) (\rho_p^2 + \rho_n^2) \right], \\
\mathcal{H}_{\text{eff}} &= \frac{1}{8} [t_1 (2 + x_1) + t_2 (2 + x_2)] \tau \rho \\
&\quad + \frac{1}{8} [t_2 (2x_2 + 1) - t_1 (2x_1 + 1)] (\tau_p \rho_p + \tau_n \rho_n), \\
\mathcal{H}_{\text{fin}} &= \frac{1}{32} [3t_1 (2 + x_1) - t_2 (2 + x_2)] (\nabla \rho)^2 \\
&\quad - \frac{1}{32} [3t_1 (2x_1 + 1) + t_2 (2x_2 + 1)] \left[(\nabla \rho_p)^2 + (\nabla \rho_n)^2 \right], \\
\mathcal{H}_{\text{so}} &= \frac{1}{2} W_0 [\mathbf{J} \cdot \nabla \rho + \mathbf{J}_p \cdot \nabla \rho_p + \mathbf{J}_n \cdot \nabla \rho_n], \\
\mathcal{H}_{\text{sg}} &= -\frac{1}{16} (t_1 x_1 + t_2 x_2) \mathbf{J}^2 + \frac{1}{16} (t_1 - t_2) [\mathbf{J}_p^2 + \mathbf{J}_n^2]. \tag{2.2}
\end{aligned}$$

Total densities are defined as $\rho = \rho_p + \rho_n$, $\tau = \tau_p + \tau_n$, $\mathbf{J} = \mathbf{J}_n + \mathbf{J}_p$. Neutron and proton ($q = n, p$) local matter densities are:

$$\rho_q(\mathbf{r}) = \sum_{i,s} |\varphi_i^q(\mathbf{r}, s)|^2 n_i^q. \tag{2.3}$$

Similarly the kinetic and the spin densities read :

$$\tau_q(\mathbf{r}) = \sum_{i,s} |\nabla \varphi_i^q(\mathbf{r}, s)|^2 n_i^q, \tag{2.4}$$

$$\mathbf{J}_q(\mathbf{r}) = \sum_{i,s,s'} \varphi_i^{q*}(\mathbf{r}, s') \nabla \varphi_i^q(\mathbf{r}, s) \times \langle s' | \boldsymbol{\sigma} | s \rangle n_i^q, \tag{2.5}$$

where $\varphi_i^q(\mathbf{r}, s)$ is the single-particle wave function with orbital, spin and isospin quantum numbers, i , s and q , respectively; and n_i^q the occupation number of the corresponding state i, s, q . Within the Hartree–Fock approximation, these single particle wave functions and their corresponding single particle energies are obtained from the self-consistent equation:

$$\begin{aligned}
&\left\{ -\nabla \frac{\hbar^2}{2m_q^*(\mathbf{r})} \cdot \nabla + U_q(\mathbf{r}) + \delta_{q,\text{proton}} V_{\text{coul}}(\mathbf{r}) - i \mathbf{W}_q(\mathbf{r}) \cdot (\nabla \times \boldsymbol{\sigma}) - e_i \right\} \\
&\quad \times \varphi_i^q(\mathbf{r}, s) = 0. \tag{2.6}
\end{aligned}$$

The effective mass $m_q^*(\mathbf{r})$, which depends upon the \mathcal{H}_{eff} part of the energy density functional, is defined as:

$$\begin{aligned}
\frac{\hbar^2}{2m_q^*(\mathbf{r})} &= \frac{\hbar^2}{2m} + \frac{1}{8} [t_1 (2 + x_1) + t_2 (2 + x_2)] \rho(\mathbf{r}) \\
&\quad - \frac{1}{8} [t_1 (1 + 2x_1) + t_2 (1 + 2x_2)] \rho_q(\mathbf{r}). \tag{2.7}
\end{aligned}$$

The nuclear central and spin–orbit fields are respectively:

$$\begin{aligned}
U_q(\mathbf{r}) &= \frac{1}{2} t_0 [(2 + x_0) \rho - (1 + 2x_0) \rho_q] \\
&\quad + \frac{1}{24} t_3 \left\{ (2 + x_3) (2 + \alpha) \rho^{\alpha+1} \right. \\
&\quad \left. - (2x_3 + 1) [2\rho^\alpha \rho_q + \alpha \rho^{\alpha-1} (\rho_p^2 + \rho_n^2)] \right\}
\end{aligned}$$

$$\begin{aligned}
& + \frac{1}{8} [t_1 (2 + x_1) + t_2 (2 + x_2)] \tau \\
& + \frac{1}{8} [t_2 (2x_2 + 1) - t_1 (2x_1 + 1)] \tau_q \\
& + \frac{1}{16} [t_2 (2 + x_2) - 3t_1 (2 + x_1)] \nabla^2 \rho \\
& + \frac{1}{16} [3t_1 (2x_1 + 1) + t_2 (2x_2 + 1)] \nabla^2 \rho_q \\
& + \frac{1}{8} (t_1 - t_2) \mathbf{J}_q - \frac{1}{8} (t_1 x_1 + t_2 x_2) \mathbf{J},
\end{aligned} \tag{2.8}$$

$$W_q(\mathbf{r}) = \frac{1}{2} W_0 (\nabla \rho + \nabla \rho_q). \tag{2.9}$$

Finally, with the Slater approximation for the exchange part, the coulomb field takes the form:

$$V_{\text{coul}}(\mathbf{r}) = \frac{e^2}{2} \int \frac{\rho_p(\mathbf{r}') d^3 r'}{|\mathbf{r} - \mathbf{r}'|} - \frac{e^2}{2} \left(\frac{3}{\pi} \right)^{1/3} \rho_p^{1/3}. \tag{2.10}$$

3. New Skyrme forces

The parametrization SLy230b presented in I is the starting point of this work where we discuss several improvements related to a more refined *protocol* as compared to what was previously done. This force was built from the following ingredients:

- a good reproduction of the saturation point of the symmetric infinite nuclear matter, i.e. $\rho_0 \simeq 0.16 \text{ fm}^{-3}$, $E/A \simeq -16 \text{ MeV}$,
- a compression modulus of the symmetric nuclear matter $K_\infty \simeq 230 \text{ MeV}$,
- a symmetry energy $a_S \simeq 32 \text{ MeV}$,
- an enhancement factor of the Thomas–Reiche–Kuhn sum rule $\kappa = 0.25$ (energy weighted sum rule occurring in the E1; $T = 1$ giant dipole resonance),
- a reasonable reproduction of the Wiringa et al. [8] equation of state for pure neutron matter,
- a good reproduction (see Table 5 in part I) of the binding energies of doubly magic nuclei – ^{16}O , $^{40,48}\text{Ca}$, ^{56}Ni , ^{132}Sn and ^{208}Pb – as well as their r.m.s. radii when experimentally known,
- no constraint on the surface properties.

In these attempts [21], the choice of the ^{16}O nucleus was mostly done for historical reasons: most of the published Skyrme forces include the binding energy and the r.m.s. radius of this nucleus in their fit. However, this light nucleus introduces a too strong constraint in the fit, especially for the r.m.s. radius. Mean field theories are better justified in the limit of a large number of nucleons. A priori, one should not include such a light system where the ground state wave function contains large correlations beyond the mean field [22,25]. Already in paper I, we had abandoned the ^{16}O nucleus to adjust the spin–orbit strength of the interaction and chosen the neutron $3p_{1/2} - 3p_{3/2}$ single particle energy splitting in ^{208}Pb , instead of the $1p$ -shell splitting in ^{16}O . We verified afterward that the results obtained for ^{16}O were not significantly different.

In the present paper, we further modify the above *protocol* by excluding all properties of ^{16}O . Furthermore we also discarded ^{78}Ni , the properties of which resulting from

Table 1

Parameters of the new Skyrme forces used in the text

	SLy4	SLy5	SLy6	SLy7	SkM*
t_0 (MeV fm ³)	−2488.91	−2484.88	−2479.50	−2482.41	−2645.00
t_1 (MeV fm ⁵)	486.82	483.13	462.18	457.97	410.00
t_2 (MeV fm ⁵)	−546.39	−549.40	−448.61	−419.85	−135.00
t_3 (MeV fm ^{3+3σ})	13777.0	13763.0	13673.0	13677.0	15595.0
x_0	0.834	0.778	0.825	0.846	0.09
x_1	−0.344	−0.328	−0.465	−0.511	0.00
x_2	−1.000	−1.000	−1.000	−1.000	0.00
x_3	1.354	1.267	1.355	1.391	0.00
σ	1/6	1/6	1/6	1/6	1/6
W_0 (MeV fm ⁵)	123.0	126.0	122.0	126.0	130.0

Table 2

Properties of symmetric infinite nuclear matter for the Skyrme effective interactions used in the text. All the properties given in this table as well as in the text have been calculated with the values given in paper I for the usual fundamental constants

Force	SLy4	SLy5	SLy6	SLy7	SkM*
ρ_∞ (fm ^{−3})	0.160	0.160	0.159	0.158	0.160
k_F (fm ^{−1})	1.333	1.334	1.330	1.328	1.334
a_c (MeV)	−15.969	−15.983	−15.920	−15.894	−15.770
K_∞ (MeV)	229.9	229.9	229.8	229.7	216.6
m_∞^*/m	0.70	0.70	0.69	0.69	0.79
a_s (MeV)	32.00	32.03	31.96	31.99	30.03
κ (E1; $T = 1$)	0.25	0.25	0.25	0.25	0.53
a_{surf} (MeV) ($Y_p = 0.5$)	18.11	18.04	17.36	17.00	17.38
a_{surf} (MeV) ($Y_p = 0.3916$)	16.67	16.56	15.98	15.66	16.01

extrapolations rather than coming from actual data. Indeed this choice, which would have been rather academic for the neutron star properties discussed in paper I, is more coherent with the spirit of a mean field approximation and proved to yield better overall agreement with spectroscopic data.

We named SLy4 the new set of Skyrme parameters resulting from the above protocol. The actual values of these parameters are listed in Table 1. Table 2 shows the corresponding properties of infinite matter. Binding energies and r.m.s. radii of the nuclei included in the fit, and also of ¹⁶O, ⁷⁸Ni and ¹⁰⁰Sn, are compared with experiment in Table 3. Let us recall that the energy and r.m.s. radius tolerances in the χ^2 fit are chosen to be 2 MeV and 0.02 fm, respectively (see paper I). One can verify on Table 3 the quality of the fit and also that the calculated binding energy and r.m.s. radius of ¹⁶O are indeed very well reproduced, even though this nucleus is not anymore included in the protocol. As we can see on these three tables, the basic parametrizations SLy4 presented here is very close to the SLy230b one presented in paper I. These three tables also include three other sets of parameters – SLy5, SLy6 and SLy7 – which we now describe.

Table 3

Binding energies (in MeV) (upper part of the table) and charge radii (in fm) (lower part of the table) of double closed shell nuclei for the Skyrme effective interactions used in the text. Results for SIII [2] and SkM* [4] interactions are given for comparison. Experimental masses are taken from Audi et al. [26]; charge experimental radii are taken from Otten [79]

	SLy4	SLy5	SLy6	SLy7	SIII	SkM*	exp
$^{16}\text{O}^a$	-128.51	-128.41	-127.28	-128.55	-128.22	-127.73	-127.62
^{40}Ca	-344.23	-344.06	-342.78	-344.90	-341.83	-341.05	-342.05
^{48}Ca	-417.87	-415.88	-416.02	-415.88	-418.15	-420.00	-415.99
^{56}Ni	-483.31	-482.65	-482.10	-482.22	-483.55	-485.35	-483.99
$^{78}\text{Ni}^a$	-643.77	-643.98	-641.78	-640.88	-646.04	-653.63	-642.40 ^b
$^{100}\text{Sn}^a$	-828.53	-827.80	-828.89	-829.63	-827.19	-826.13	-825.78
^{132}Sn	-1103.43	-1103.85	-1103.19	-1102.77	-1105.65	-1110.48	-1102.90
^{208}Pb	-1635.55	-1636.02	-1636.53	-1636.76	-1636.35	-1636.15	-1636.44
$^{16}\text{O}^a$	2.779	2.777	2.752	2.747	2.733	2.787	2.73
^{40}Ca	3.493	3.489	3.472	3.470	3.480	3.499	3.49
^{48}Ca	3.511	3.507	3.493	3.495	3.520	3.504	3.48
^{56}Ni	3.772	3.766	3.753	3.758	3.788	3.758	3.75
$^{78}\text{Ni}^a$	3.970	3.962	3.960	3.967	4.007	3.958	^c
$^{100}\text{Sn}^a$	4.487	4.480	4.471	4.476	4.522	4.480	^c
^{132}Sn	4.715	4.706	4.706	4.713	4.768	4.705	^c
^{208}Pb	5.498	5.488	5.490	5.498	5.561	5.492	5.50

^a Nucleus not included in our *protocol*.

^b Extrapolated value [26].

^c No experimental data.

3.1. J^2 terms

The energy density functional (Eq. (2.2)) contains a \mathcal{H}_{sg} term which results from the coupling of the spin with the gradient operator occurring in the expression of the two-body interaction. This term vanishes for spin saturated systems where the spin density $J_q(\mathbf{r})$ is equal to zero. For this reason, and also because the corresponding contribution to the one-body hamiltonian of the mean field was difficult to calculate especially for deformed nuclei, most of the previously proposed Skyrme forces have neglected this term [2,4,19]. When calculated in first order perturbation, the order of magnitude of this term is typically 6 MeV in ^{208}Pb . We have verified numerically that it does not depend very much upon collective degrees of freedom such as quadrupole or octupole deformations over a wide range of variation. We have anyhow decided to investigate its importance. For that purpose, we have included it in the energy functional and rerun the fitting procedure, the resulting parameters are named SLy5. Tables 1–3 give its parameters, infinite nuclear matter and finite nuclei properties, respectively.

3.2. Center of mass correlations (or corrections)

In Hartree–Fock calculations the center of mass (c.m.) motion generates spurious states and its contribution to the energy must be extracted. This is done by replacing in the two-body Hamiltonian, the kinetic operator K by:

Table 4

Constraints used for the new Skyrme forces

	SLy4	SLy5	SLy6	SLy7	SLy10
UV14+UVII EOS ^a	×	×	×	×	×
Binding energies and $\langle r^2 \rangle_{\text{ch}}$	×	×	×	×	×
Splitting $3p_{\frac{1}{2}} - 3p_{\frac{3}{2}}$ in ^{208}Pb	×	×	×	×	×
$x_2 = -1$ ^b	×	×	×	×	×
J^2 terms		×		×	×
Two-body cm correction			×	×	×
Two components in spin-orbit					×

^a See paper I, Section 3.3 for the discussion of these constraints.^b See paper I, Section 3.6 for the discussion of these constraints.

$$K - \frac{P^2}{2mA} = K - \frac{(\sum_i \mathbf{p}_i)^2}{2mA} = K - \frac{1}{2mA} \left[\sum_i p_i^2 + \sum_{i \neq j} \mathbf{p}_i \cdot \mathbf{p}_j \right]. \quad (3.1)$$

Traditionally, only the one-body correction term is taken into account. It yields an adding term $-1/A$ in the kinetic energy term. The second term is a two-body term and is more difficult to evaluate. Its direct part vanishes, and only the exchange contribution is non-zero. It is thus expected to be small and has been neglected so far. However, when calculated in perturbation, it contributes for about 13 MeV in ^{208}Pb . As for the \mathcal{H}_{sg} term, we have verified numerically that it does not vary significantly with deformations. Nevertheless such a term may induce some correlations which can be important in a detailed analysis of isotopic shifts. It also may affect the adjustment of the spin-orbit strength [27]. We have therefore decided to study this term. The SLy6 set of parameters listed in Table 1 has been obtained with this two-body c.m. correction included in the energy functional.

With both the spin-gradient and the two-body c.m. contributions included, we have obtained a fourth set of parameters: SLy7. Tables 1–3 summarize the parameters and properties of these four new forces. Table 4 presents the corresponding terms included in the protocol. Of course, to use interactions such as SLy5, SLy6 or SLy7, one should have a Hartree–Fock program which includes these extra terms explicitly in the non-linear self-consistent algorithm. If such codes are not available, one should calculate these terms perturbatively.

4. Results

In the present work we have limited ourselves to spherical calculations in order to compare our new force with SkM* which we use as a reference. Further studies will be devoted to deformation properties. Some results with SLy4 have already been obtained in an extensive study of super deformed rotational bands in the $A = 150$ mass region [28]. As most of the available Hartree–Fock programs are designed without the spin-gradient and the two-body c.m. contribution, we have singled out SLy4 in the following sections.

To calculate spectroscopic properties of nuclei away from the magic nuclei included in our protocol, we have defined a two-body interaction to be used in the particle-particle channel.

4.1. Pairing correlations

Recent calculations of isotopic shifts have shown that pairing correlations depend strongly upon the structure of the force [29]. Several other studies have also indicated that a density dependent delta interaction provides better agreement with experiment [30,33].

We have included pairing correlations in the BCS approximation, using a density dependent zero-range force:

$$V_P = \frac{V_0}{2} (1 - P_\sigma) \left(1 - \frac{\rho(r_1)}{\rho_c} \right) \delta(r_1 - r_2), \quad (4.1)$$

where the critical density ρ_c is equal to 0.16 fm^{-3} . The strength V_0 has been fixed equal to 1000 MeV fm^3 for SLy4 to SLy7, and to 880 MeV fm^3 for SkM*. The actual value of this parameter depends upon the level density around the Fermi energy. In order to avoid divergences, the definition of the force involves also an energy cut-off parameter in the valence single-particle space to limit the active pairing space above the Fermi level to one major shell. In the present study we have used the cut-off prescription defined in Ref. [34].

4.2. Binding energies and single particle spectra

Fig. 1 shows the isotopic energy differences ΔE for the Ni isotopes calculated with SLy4 and SkM*:

$$\Delta E = [E - E(^{56}\text{Ni})]_{\text{HFBCS}} - [E - E(^{56}\text{Ni})]_{\text{exp}}. \quad (4.2)$$

For these rather light nuclei, no significant differences are observed between the two forces. However, ground state correlations and/or deformations may play an important role, especially for the heaviest isotopes.

Similar results for Sn isotopes are shown on Fig. 2 and for $N = 82$ isotones on Fig. 3. For these heavier nuclei, the improvement obtained with our new SLy4 set of parameters is quite remarkable. In the original derivation of SkM* parametrization [4], the deviation with experiment for the heaviest Sn isotopes was already reported, SLy4 seems to have resolved this discrepancy. The results presented here use a density dependent zero range pairing interaction which produces significant improvement of the treatment of these correlations compared to the G -constant recipe previously used. We have checked that SLy4 is responsible of most of the overall improvements of the results [21]. The new choice for the pairing interaction brings only additional refinements.

We have also calculated the Pb isotopes, Fig. 4 compares our results with SkM*. Even though SkM* results are slightly better for isotopes heavier than ^{208}Pb , the overall agreement is in favor on SLy4.

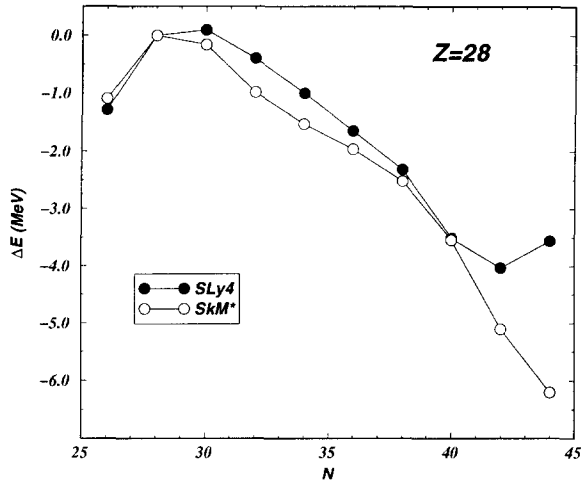


Fig. 1. Isotopic energy differences $\Delta E = |E - E(^{56}\text{Ni})|_{\text{HFBCS}} - |E - E(^{56}\text{Ni})|_{\text{exp}}$ (in MeV) as a function of the neutron number N for Ni isotopes. The results for the new SLy4 parametrization is compared to the SkM* ones.

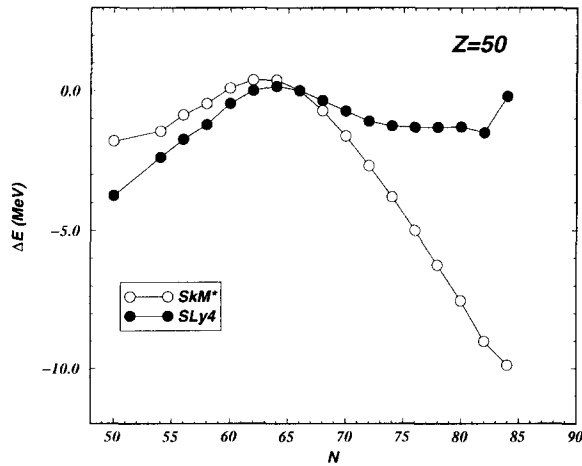


Fig. 2. Same as Fig. 1 for tin isotopes. ^{116}Sn is taken as reference.

In the above comparison we have arbitrarily limited ourselves to nuclei with experimentally known binding energies, leaving out standard extrapolations such as [18]. As a result the commonly observed *arches* for ΔE (see for example Ref. [35]) in between magic numbers are only seen in lead isotopes. In these nuclei the *arch* amplitude is significantly reduced for SLy4, in spite of the rise beyond $N = 126$. Similarly in tin isotopes the most neutron rich nucleus shows the beginning of the *arch* following $N = 82$ (see Fig. 2).

For ^{208}Pb , Fig. 5 gives the neutron and proton spectra for our forces together with the results of SIII and SkM*. As a reference, experimental values are also shown [19]. All calculated spectra are less compressed than experimental ones. This usual feature

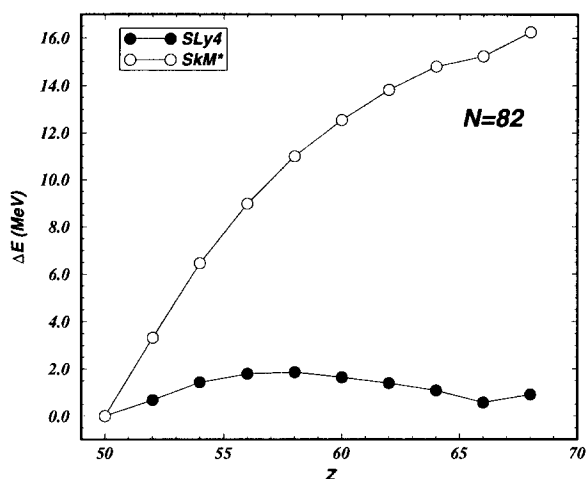


Fig. 3. Same as Fig. 1 for $N = 82$ isotones. ^{132}Sn is taken as reference.

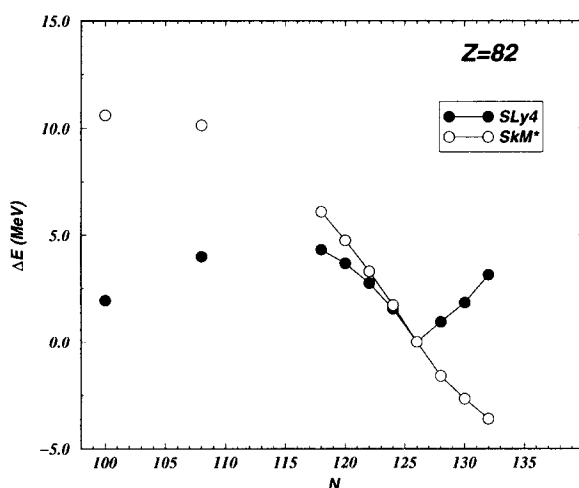


Fig. 4. Same as Fig. 1 for lead isotopes. ^{208}Pb is taken as reference.

does not reflect a weakness of any of these effective forces since correlations beyond the mean field are known to resolve this discrepancy. Indeed Nguyen Van Giai and Bernard [36] have shown that, when RPA correlations are taken into account, the comparison with experiment becomes satisfactory. Apart from the above comment, no significant differences can be observed between the different calculated spectra. Some tentative investigations have been made to connect the isospin dependence of the effective mass with the formation of a neutron skin in a neutron rich nucleus [37,38]. A clear conclusion could be made in the next future if recent experimental results obtained for light nuclei [39] are extended in a wide range of medium and heavy nuclei.

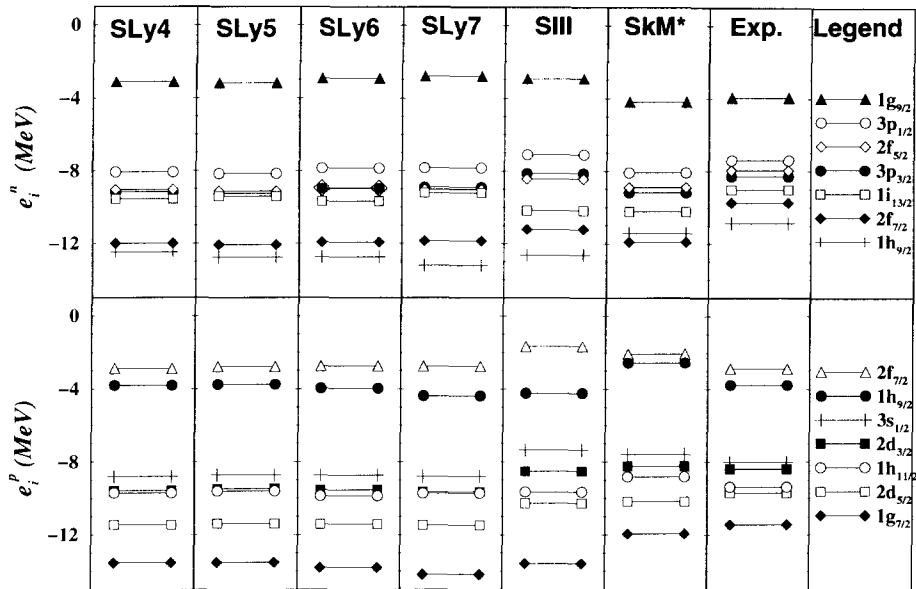


Fig. 5. Neutron (upper part) and proton (lower part) single particle spectra for ^{208}Pb calculated with SLy4, SLy5, SLy6 and SLy7. Comparison is made with SIII and SkM*. Experimental spectra [19] are also given for reference.

4.3. Isotopic shifts

Isotopic shifts have been studied for Pb isotopes (see for instance Refs. [29,40,42]). Standard effective forces, zero range or finite range ones, are not able to reproduce the observed kink. In Ref. [29] it has been shown that calculated shifts are very sensitive to the choice of the pairing interaction. Relativistic mean field calculations [40,41] were able to reproduce the data by changing some input parameters. As nuclear radii are sensitive to ground state correlations [22,42], it may be a solution to use the effective character of the interaction to slightly modify some of its parameters to improve the calculation.

In the present work we decided to calculate the Pb isotopic shifts with our new SLy4 and to investigate the effect of the spin-gradient terms (SLy5), of the two-body center of mass correction (SLy6), and of both terms simultaneously (SLy7). Such approach gives a hint on what terms are important for these radii.

Fig. 6 shows the isotopic shifts calculated with SLy4 and SkM* compared to the experiment. The results obtained with SLy4 are slightly better than those obtained with SkM*. While the calculations by Tajima et al. [29] use the SkM* force with a G -constant pairing interaction, the two calculations presented here use the density dependent delta interaction described in Section 4.1 and the difference between the two results is unambiguously due to the force.

Fig. 7 displays the results obtained with our four new forces compared with experiment. The sole effect of the spin-gradient terms is not very important: SLy5 results are

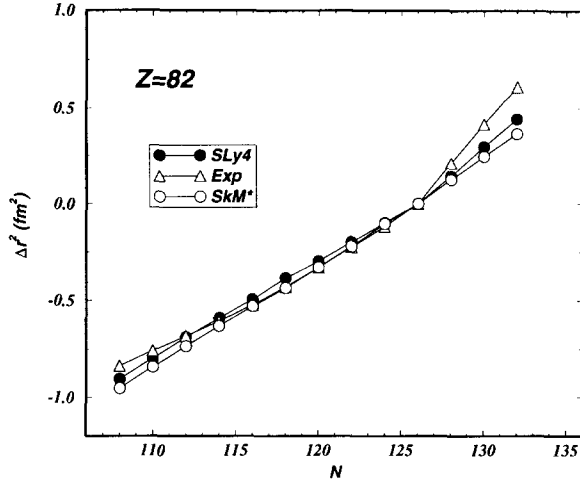


Fig. 6. Isotopic shifts $\Delta r^2 = [\langle r^2 \rangle - \langle r^2 \rangle(^{208}\text{Pb})]$ (in fm^2) for lead isotopes. Results for the two SLy4 and SkM* forces are compared to the experiment [79].

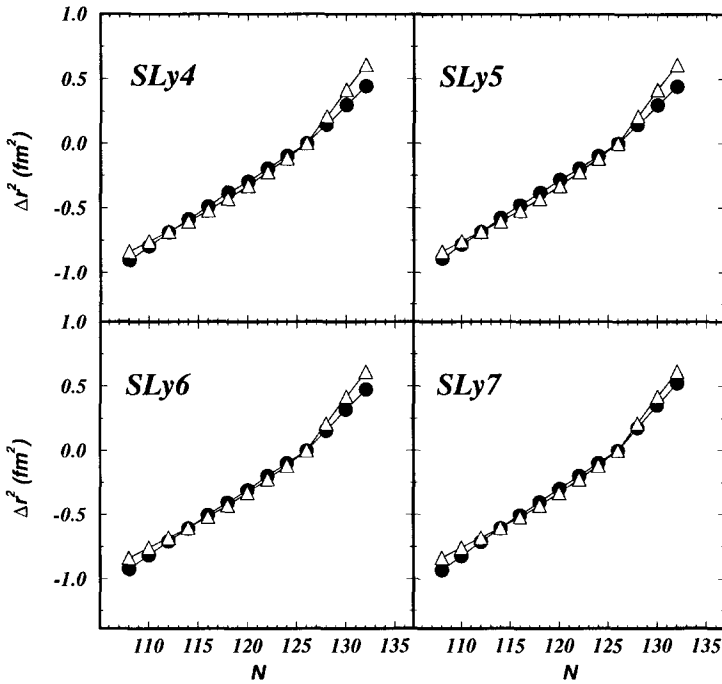


Fig. 7. Same as Fig. 6 with the different SLy4 to SLy7 Skyrme forces (black circles) compared to the experimental results (open triangles).

quite similar to those of SLy4. The two-body c.m. correction alone improves slightly the results (SLy6 as compared to SLy4). In contrast, the joint contribution of the two terms (SLy7) brings significant improvement. Fig. 8 shows that the corresponding ΔE are not modified significantly from the SLy4 to the SLy7 parametrization, confirming

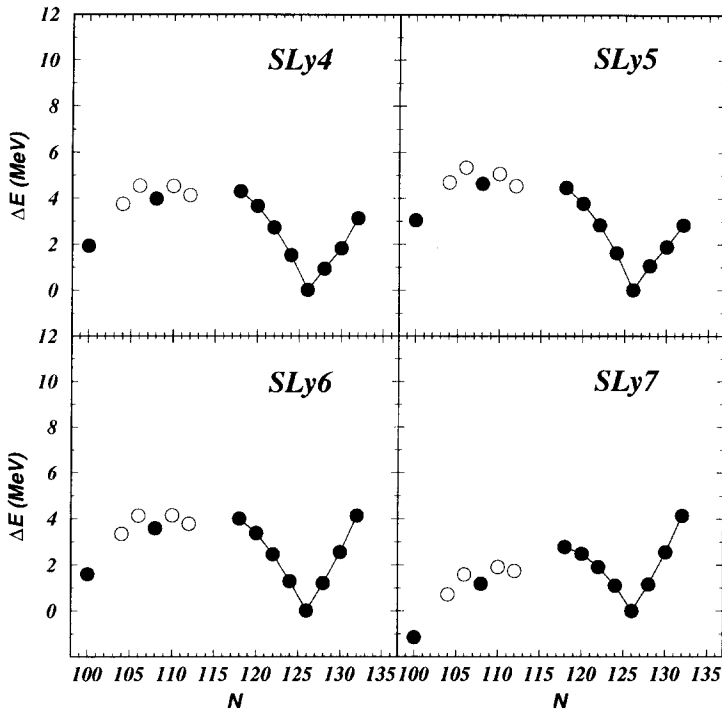


Fig. 8. Isotopic energy differences ΔE (in MeV) (see Fig. 1 for the definition) corresponding to the isotopic shifts of Fig. 7. Open circles correspond to ΔE calculated with extrapolated masses instead of experimental ones [18].

thus our previous conclusions about the isotopic shifts. From this analysis, we think that calculations aiming at reproducing accurately the nuclear radii ought to include these terms at the mean field level, especially the two-body center of mass correction. This last term does not depend upon the choice of the parameter of the interaction. This does not preclude possible contributions coming from ground state correlations.

4.4. Towards the drip lines

We have calculated the two neutron separation energies up to the drip line for several isotopic chains. At the present time, these calculations have been done within the BCS approximation for the pairing correlations. Near the drip line, continuum states are populated. It has been shown that full Hartree–Fock–Bogoliubov (HFB) methods resolve the difficulty arising from continuum states, provided the chemical potential remains negative [10,43]. In our case however, calculations are performed in a spherical basis and it is possible to carefully select the relevant single particle states which are quasi-bound states because of their own centrifugal barrier. We are quite aware that our calculations should be confirmed by full HFB calculations close to the drip line. However, in the isotopic chain we have studied, we think that BCS calculations provide a good qualitative estimate of the position of the drip line as discussed below.

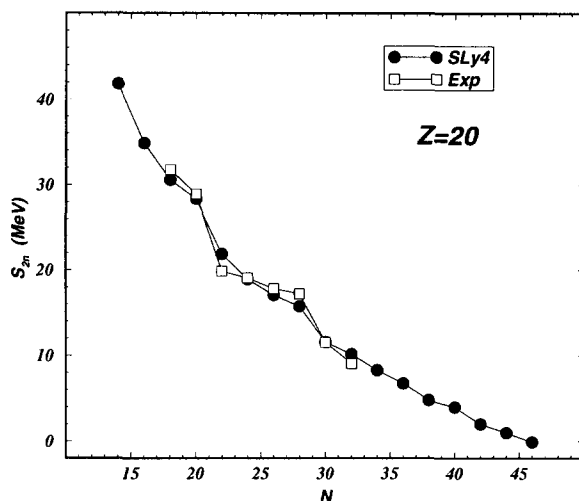


Fig. 9. S_{2n} two neutron separation energies for Calcium isotopes calculated with SLy4 (solid circles) compared with experiment (open squares).

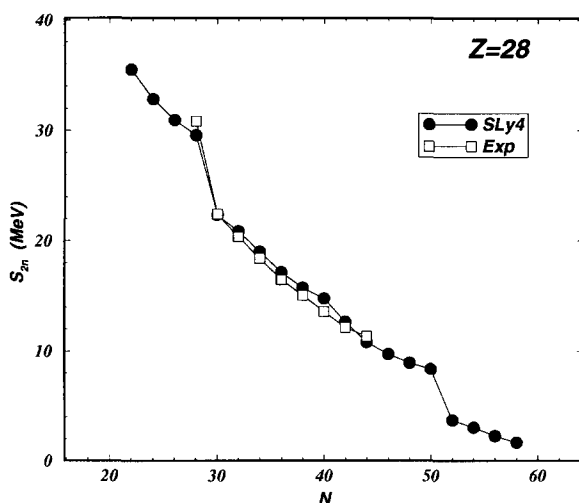


Fig. 10. Same as Fig. 9 for nickel isotopes.

Figs. 9–12 show the results obtained with the basic force SLy4 for the two neutron separation energies, S_{2n} , for the isotopic series of magic nuclei, namely Ca, Ni, Sn and Pb. For Ca and Ni isotopes, the agreement with experiment is rather good, Ca two neutron drip line is predicted to lie at $N = 46$, i.e. $^{66}_{20}\text{Ca}$. For Ni isotopes, we have not reached the drip line. However, up to $N = 58$, our results are comparable to the full HFB calculations of Ref. [43] performed with the SIII interaction [2] and which predict the neutron drip line at $N = 64$, i.e. $^{92}_{28}\text{Ni}$.

For the Sn isotopes (see Fig. 11), we have a good agreement with experiment up to neutron number $N = 82$, however SLy4 overestimates the shell effect at the magic

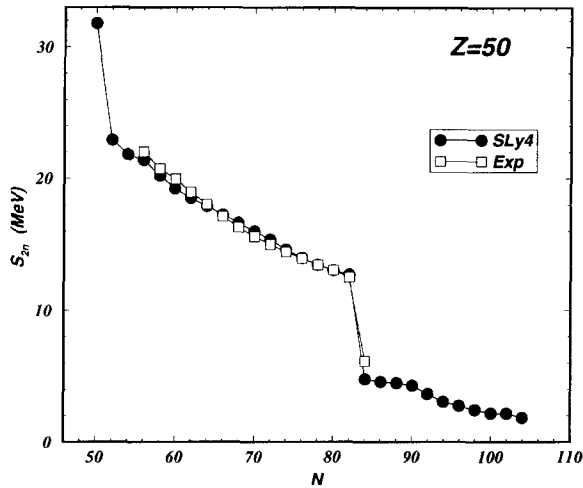


Fig. 11. Same as Fig. 9 for tin isotopes.

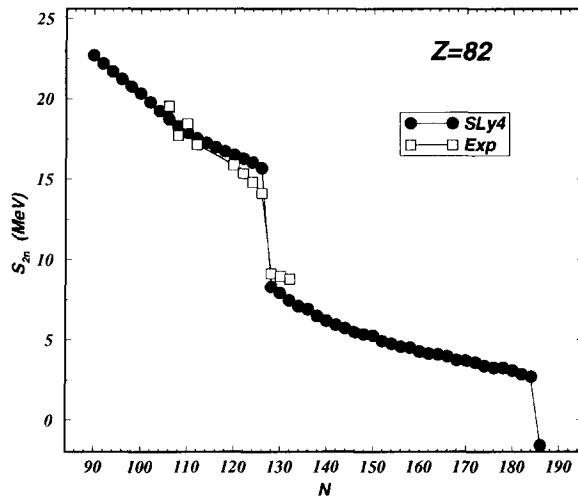


Fig. 12. Same as Fig. 9 for lead isotopes.

number $N = 82$. The predicted shell effect is also too large for Pb isotopes around the magic number $N = 126$ (see Fig. 12). Next magic number is expected to be $N = 182$. To actually reach the drip line, one should indeed performed full HFB calculations.

We have also calculated two proton separation energies, S_{2p} , for the $N = 82$ isotonic chain, results are shown on Fig. 13. The agreement with experiment is good, unfortunately there is no experimental data to check whether the shell effect at $Z = 50$ is correctly predicted or overestimated as for the neutron case. The proton drip line is reached for the $^{156}_{74}\text{W}$ isotone, in qualitative agreement with experiment [44]. Close to the proton drip line, single particle states relevant for pairing correlations are either bound or quasi bound by the coulomb field so that the BCS approximation remains well

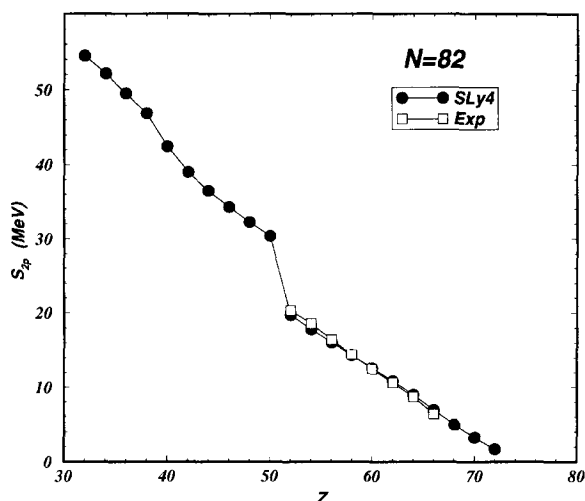


Fig. 13. S_{2p} two proton separation energies for the $N = 82$ serie of isotones calculated with SLy4 (solid circles) compared with experiment (open squares).

justified. This is indeed why we were able to actually reach the proton drip line in our calculations.

As compared to calculations with other forces [10,45,46] the calculated S_{2n} and S_{2p} with SLy4 definitively improve upon those obtained with SkM* [4]. Our results are somewhat comparable to those of the Skyrme SkP parametrization [47].

The above results are sufficient to assess the ability of the SLy4 interaction to make relevant predictions away from the stability line. A complete search of the proton and neutron drip lines is beyond the scope of the present work.

5. Surface properties

In paper I we proposed to characterize the surface properties of these new forces by a single coefficient a_{surf} (see for example Ref. [48] and references therein for the discussion about the two surface and surface-symmetry terms involved in a_{surf}). This coefficient is obtained in a semi classical calculation of a slab of semi-infinite nuclear matter using standard Extended Thomas–Fermi techniques [49,51]. For asymmetric matter, this coefficient will depend upon the proton fraction $Y_p = Z/A$ and our calculation will be restricted to the values of Y_p around the normal nuclear matter. The surface properties around the pure neutron matter and probably also around the neutron drip line should be examined in a more sophisticated model [52,53]. Table 2 gives a_{surf} for symmetric matter ($Y_p = 0.5$) and for an asymmetric matter corresponding to the proton fraction of ^{240}Pu ($Y_p = 0.3916$).

One of the most severe test of the surface tension of an effective force is the analysis of fission barriers. Indeed fission isomers have very deformed ellipsoidal shapes with an axis ratio of 2 : 1. Their excitation energies thus depend not only upon the shell effects

Table 5

Surface tension, first barrier height and excitation energy (in MeV) of the isomeric state of ^{240}Pu

	a_{surf}	$E(\text{barrier})$	$E(\text{2nd minimum})$
SLy4	16.67	11.6	5.1
SkM*	16.01	10.4	3.2
SLy7	15.66	9.9	3.0

which create the secondary minimum but also upon the surface tension.

Axial fission barrier of ^{240}Pu has been extensively studied, e.g. with the SkM* interaction whose surface tension has been adjusted onto this nucleus [4]. We have therefore decided to use ^{240}Pu as a test case and to perform a full three dimensional Hartree–Fock plus BCS calculation of the height of the axial barrier between the ground state and the secondary minimum, as well as the excitation energy of the isomeric state. These results are reported in Table 5 together with the corresponding surface tension. A more complete study of the shapes of the fission barriers in the actinide region is under progress. Preliminary results can be found in Ref. [12].

From Table 5, one observes a definite correlation between the surface tension a_{surf} and the excitation energy of the second well. Even though the determination of a_{surf} is model dependent, its relative magnitude between different forces seems to be meaningful. Indeed though SLy7 differs from SLy4 by the spin-gradient and the two-body center of mass terms, we think that the above correlation is quite relevant as the contributions of these two terms do not depend very significantly over the studied range of deformations. In the χ^2 , no constraint on a_{surf} was included. The parametrization SLy4 and SLy7 have somewhat adjusted themselves at two different locations in the rather shallow minima in the multi parameter variational space in which the minimization algorithm is performed. Finally, the value of a_{surf} could be used to constrain the force if need be.

6. Spin–orbit term

Spin–orbit term plays probably a crucial role to drive the shell effects far for the stability line. The robustness of magic numbers near the neutron drip line will depend strongly upon this term and thus upon the parametrization of this term in a non-relativistic effective interaction. Relativistic approaches of this part of the force lead to a drastic decreasing of the spin–orbit strength when increasing the neutron excess [54]. This effect has been investigated in light [55,56] and medium [57] neutron rich nuclei as well as near the proton drip line [58] with a softer amplitude.

In our new forces we have used the standard form of the spin–orbit term (see Eq. (2.1) in paper I). (Notice that the same form is also used in addition to the Gogny force [59,60] when one uses usual finite-range effective forces).

Relativistic Mean Field (RMF) theories gives a natural framework to generate the spin–orbit field where it appears as a consequence of the Lorentz invariance of the theory. Non-relativistic limits of these theories have been studied in order to extract

Table 6

Parameters and nuclear matter properties of the SLy10 Skyrme force

t_0 (MeV fm ³)	−2506.77	ρ_∞ (fm ^{−3})	0.156
t_1 (MeV fm ⁵)	430.98	k_F (fm ^{−1})	1.322
t_2 (MeV fm ⁵)	−304.95	a_v (MeV)	−15.901
t_3 (MeV fm ^{3+3σ})	13826.41	K_∞ (MeV)	229.7
x_0	1.0398	m_∞^*/m	0.68
x_1	−0.6745	a_s (MeV)	31.98
x_2	−1.000	κ (E1; T = 1)	0.25
x_3	1.6833		
σ	1/6		
W_1 (MeV fm ⁵)	75.86		
W_2 (MeV fm ⁵)	105.50		

some insights about the spin–orbit field which is included in any non-relativistic Hartree–Fock theories [61,41] based upon effective nucleon–nucleon forces. In these limits, the resulting energy density functional is more complicated than that usually included in mean field calculations. More general effective field theories expect for example a direct connection between spin–orbit splittings and the effective mass of the nucleon [63,64]. In a simple phenomenological way, several propositions have been made [41,65] which consist to have different form factors for neutrons and protons following an idea already expressed by Dabrowski [66]. Reinhard and Flocard [67] have recently proposed to use a two components spin–orbit contribution of the following form:

$$\mathcal{H}_{\text{so}} = \frac{W_1}{2} \mathbf{J} \cdot \nabla \rho + \frac{W_2}{2} \{ \mathbf{J}_p \cdot \nabla \rho_p + \mathbf{J}_n \cdot \nabla \rho_n \}, \quad (6.1)$$

where one recovers the standard functional for $W_1 = W_2$. The case $W_2 = 0$ corresponds to the non-relativistic limit of RMF theories.

Following this suggestion, we have introduced this new parametrization of the spin–orbit term. We have kept the $3p$ spin–orbit splitting in our *protocol* and added the value of the kink angle of the lead isotopic shifts. This gave us a new set of Skyrme parameters together with W_1 and W_2 which we called SLy10. The parameters and the nuclear matter properties of this new parametrization are given in the Table 6. In the derivation of SLy10, the spin-gradient and two-body c.m. terms are taken into account, as in SLy7. Fig. 14 shows the results for the isotopic shifts of lead isotopes compared to those obtained with SLy7.

However, we must mention the work of Tajima et al. [29] who were also able to improve upon the isotopic trend for lead isotopes with a standard spin–orbit interaction. Even though the overall trend of the isotopic shifts was not correct, Tajima et al. [29] were able to reproduce the magnitude of the observed kink across ²⁰⁸Pb while adjusting carefully the pairing field with a delta density dependent interaction.

To summarize these different approaches, we can say that RMF calculations suggest that the analytical structure of the spin–orbit effective interaction in the non-relativistic limit should be revisited. This is strongly supported by the RMF calculations themselves [55,58] together with the work of Ref. [67] as well as with our exploratory

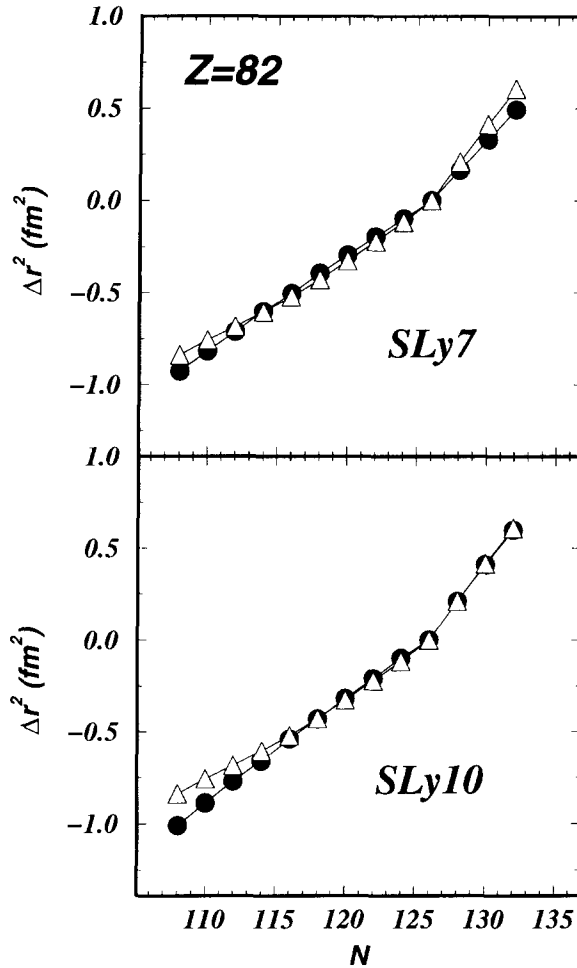


Fig. 14. Isotopic shifts (see Fig. 6 for the definition) in lead isotopes obtained for the two SLy7 and SLy10 Skyrme forces.

calculation with the SLy10 interaction.

On the other hand, the work of Tajima et al. [29] shows that the adjustment of such a new spin-orbit field cannot be done independently of a readjustment of the pairing field. Both parts of the interaction affect and depend crucially upon the details of single spectra in the vicinity of the Fermi energy.

At the present time there is no well defined *protocol* which implements in a non-ambiguous way the spin-orbit and the pairing fields to derive new forces. Furthermore, the derivation of our SLy7 force shows that such a *protocol* will have to include two-body center of mass correction. To our knowledge these center of mass corrections are not included in RMF approaches.

In the absence of such a new *protocol*, our new forces represent a significant improvement over earlier Skyrme-like interactions.

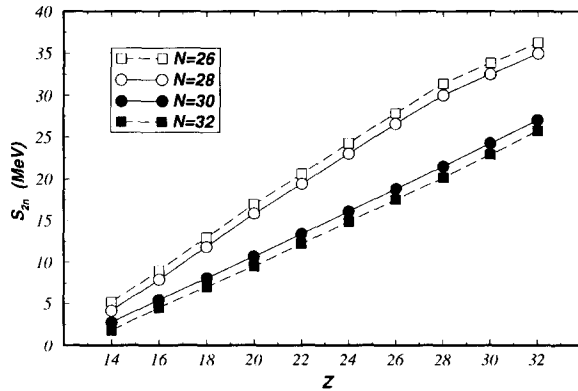


Fig. 15. Shell effects for the $N = 28$ number of neutrons as a function of the Z proton number for the SLy4 parametrization.

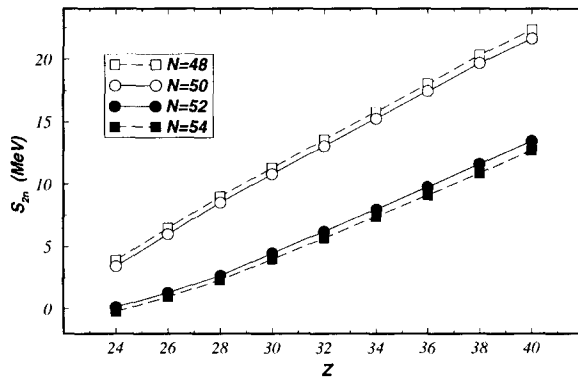


Fig. 16. Same as Fig. 15 for $N = 50$.

7. Shell effects near the neutron drip line

Shell effects associated to magic numbers are usually thought to decrease when approaching the neutron drip line. This quenching has important consequences for the description of the astrophysical r -process [68]. We have done some preliminary calculations to check whether such a feature was also predicted with the SLy4 force.

The behavior of the two-neutron separation energies as a function of the proton number around the $N = 28$, $N = 50$ and $N = 82$ are displayed respectively on Fig. 15–17.

Our results are similar to those obtained by Dobaczewski et al. [10] which predicts a decrease of the shell effects near the neutron drip line for $N = 28$ neutron number. This effect has been noticed for ^{44}S [69] and recently confirmed by exhaustive RMF calculations of neutron-rich isotopes in the $Z = 10$ – 22 region [70] as well as by shell model calculations with a smaller amplitude [71]. This is a further confirmation of the weakness of the magicity far from the stability line which has been also investigated experimentally at GANIL [72,73] and at MSU [74] where moderate deformations have been found in this region.

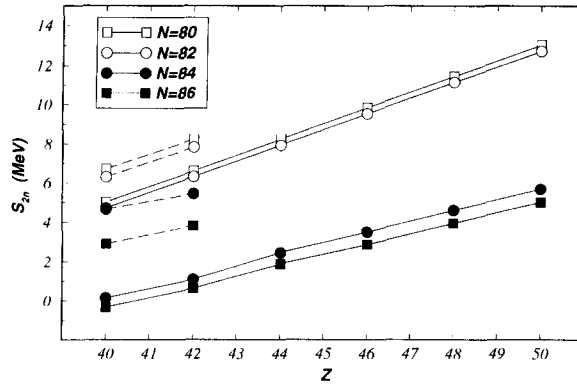


Fig. 17. Same as Fig. 15 for $N = 82$. Full line curves correspond to the SLy4 force. Dotted line curves correspond to the SkM* parametrization and they are limited to strontium and zirconium isotopes.

Fig. 16 shows that even if one observes a soft quenching of the shell effects for $N = 50$ neutron number, it seems that $N = 50$ remains a robust magic number around the neutron drip line.

This is also the case for the $N = 82$ neutron number as one can see on Fig. 17. This figure shows also for comparison a part of the effect, especially around the ^{122}Zr nucleus, obtained with the SkM* effective interaction. This latter force exhibit a strong quenching of this $N = 82$ neutron number in contradiction with the SLy4 behavior. Using an effective force with a correct isospin dependence, such as the SLy4 force, our prediction concerning the robustness of the $N = 82$ magic number near the neutron drip line is fully coherent with the one made by RMF calculations [75]. Our results give an answer to the controversy that existed between RMF and Skyrme Hartree–Fock calculations about the availability of such interactions for exotic nuclei [75].

8. Conclusions

An adjustment of the isotopic properties of the interaction solely based on the liquid drop (model) symmetry energy provides forces valid in a mass region limited to the vicinity of the β -stability line. Indeed, such a procedure relies on a local expansion of the nuclear binding energy in $I = (N - Z)/A$. To extend the validity of the force to more exotic nuclei, we have proposed to adjust the parameters on the interaction to the very extreme case of pure neutron matter. Even though the neutron equations of state remains based on theoretical derivation and has little experimental ground, we think we have demonstrated that the *protocol* we designed accordingly does repair the deficiencies of older interactions away from the stability line. Our new SLy4 interaction is a basic example of such a force which has better isotopic properties. We propose thus this new force as a good candidate to describe spectroscopic properties of nuclei from the β -stability line to the drip lines, and also other exotic phenomenon such as super- or hyper-deformation.

The other proposed forces, SLy5, SLy6 and SLy7, are to be used when the spin-gradient terms, the two-body center of mass correction term, or both are included in the Skyrme functional. Our analysis of the isotopic shifts in lead isotopes indicates that these terms should be included. Unfortunately, most of the available Hartree–Fock calculations do not include them. This is why for the sake of comparison we present SLy4 as the basic interaction, keeping in mind that our work strongly suggests that at least two-body center of mass corrections should be included future programs, as we did.

Let us emphasize that this study was done at the mean-field (Hartree–Fock) level. However, no ingredient in our *protocol* prevents further studies beyond the mean field approximation. If need be, further correlations can be explored and it is quite legitimate to use these interactions for RPA or configuration mixing (GCM) calculations. This would not have been the case if we had included in our *protocol* detailed information such as single particle energies of some selected nuclei.

All our work is based on the *standard* Skyrme functional. We do not have encountered any physical situation where this parametrization failed. There exists *non-standard* parametrizations with extra terms added to the functional, unfortunately all available ones produce some collapses in the equation of states of nuclear and/or neutron matter. These collapses occur generally at densities larger than the saturation density. Nevertheless, scaling description of the breathing mode or time dependent approaches of heavy ion collisions take into account compression effects around $\rho/\rho_0 \simeq 1.2$ and up to 1.4–1.5 for the latter [76,78]. However, due to their potential richness, the extra terms introduced in these alternate Skyrme functionals are probably worth some detailed analysis. Our *protocol* provides a natural way to explore them. For example it might be interesting to have a density dependent term $-t_3$ term – with an isospin dependence. However, it is important to include first simpler correlations such as the two-body center of mass correction. Similarly the pairing force in the particle–particle channel must be treated as accurately as possible. Otherwise a possible success of a more sophisticated parametrization might very well hide deficiencies inherent to a bad treatment of pairing or an inaccurate account of the center of mass motion.

The relativistic mean field formalism is a natural framework to take into account the spin degree of freedom. However, it suffers also from a high degree of phenomenology in the determination of its parameters. From this scheme we have a way to infer modifications to the spin–orbit term of the Skyrme functional which is probably the most weakly established term in the Skyrme effective force. The ansatz proposed by Reinhard and Flocard seems to be excellent, when used in conjunction with a full center of mass correction. Pairing correlations should be introduced through a zero-range interaction with a density dependent form factor which localizes their effects around the Fermi surface. Studies of superdeformed rotational bands have illustrated this point.

Surface properties should also be under control. A lot of works have proved that the liquid drop model or droplet model terms are too strongly model dependent to be used to constrain the determination of the parameters of the interaction. Nevertheless

this is a fundamental property for super- and hyper-deformation studies. For example if one want to investigate new superdeformation islands very far from the β -stability line, surface *and* isospin properties must be carefully adjusted. All the parametrizations proposed here have a surface energy a little higher than the SkM* one (16.3 MeV vs 16.0 MeV). The calculation of the ^{240}Pu fission barrier we have performed seems to indicate that there might be room for further improvement of the force. Similarly we have imposed in the fit a value of 230 MeV for the incompressibility modulus. Forces with a slightly reduced value, 210 MeV for instance, could be explored.

Acknowledgements

We thank C. Baktash, J.-F. Berger, R. Bougault, E. Caurier, J. Dobaczewski, H. Flocard, F. Gulminelli, P.-H. Heenen, W. Nazarewicz, P.-G. Reinhard, T. Suomijärvi and D. Vautherin for stimulating discussions during this work. When using the new forces in some various regions of nuclei and in some various applications of mean field theories, they have contributed to the achievement of this work. We thank also G. Audi for private communication of the most recent experimental or estimated masses. Part of the numerical calculations were carried out with the CRAY vector facilities of the IDRIS-CNRS Center.

References

- [1] E. Chabanat, P. Bonche, P. Haensel, J. Meyer and R. Schaeffer, Nucl. Phys. A 627 (1997) 710.
- [2] M. Beiner, H. Flocard, Nguyen Van Giai and Ph. Quentin, Nucl. Phys. A 238 (1975) 29.
- [3] H. Krivine, J. Treiner and O. Bohigas, Nucl. Phys. A 366 (1980) 155.
- [4] J. Bartel, Ph. Quentin, M. Brack, C. Guet and H.-B. Håkansson, Nucl. Phys. A 386 (1982) 79.
- [5] F. Tondeur, Nucl. Phys. A 442 (1985) 460.
- [6] M. Rayet, M. Arnould, F. Tondeur and G. Paulus, Astron. Astrophys. 116 (1982) 183.
- [7] D.G. Ravenhall, C.D. Bennett and C.J. Pethick, Phys. Rev. Lett. 28 (1972) 978.
- [8] R.B. Wiringa, V. Fiks and A. Fabrocini, Phys. Rev. C 38 (1988) 1010.
- [9] W. Nazarewicz, J. Dobaczewski, T.R. Werner, J.A. Maruhn, P.-G. Reinhard, K. Rutz, C.R. Chinn, A.S. Umar and M.R. Strayer, Phys. Rev. C 53 (1996) 740.
- [10] J. Dobaczewski, W. Nazarewicz, T.R. Werner, J.F. Berger, C.R. Chinn and J. Dechargé, Phys. Rev. C 53 (1996) 2809.
- [11] K. Rutz, M. Bender, T. Bürvenich, T. Schilling, P.-G. Reinhard, J.A. Maruhn and W. Greiner, Phys. Rev. C 56 (1997) 238;
T. Bürvenich, K. Rutz, M. Bender, P.-G. Reinhard, J.A. Maruhn and W. Greiner, submitted to Europ. Phys. J. D.
- [12] P.-H. Heenen, J. Dobaczewski, W. Nazarewicz, P. Bonche and T.L. Khoo, Phys. Rev. C (1998) in print.
- [13] M. Bender, K. Rutz, T. Bürvenich, T. Schilling, P.-G. Reinhard, J.A. Maruhn and W. Greiner, Proc. Tours Symposium on Nuclear Physics III, Tours, France, September 1997, ed. H. Utsunomiya (AIP, 1998), to be published;
M. Bender, K. Rutz, T. Bürvenich, P.-G. Reinhard, J.A. Maruhn and W. Greiner, Proc. Int. Conf. on Fission and Properties of Neutron-Rich Nuclei, Sanibel Island, Florida, USA, November 1997 (World Scientific, 1998), to be published;
M. Bender, K. Rutz, T. Bürvenich, P.-G. Reinhard, J.A. Maruhn and W. Greiner, review to be published in Heavy-Ion Physics, 1998.

- [14] D. Rudolph, C. Baktash, J. Dobaczewski, W. Nazarewicz, W. Satuła, M.J. Brinkman, M. Devlin, H.-Q. Jin, D.R. LaFosse, L.L. Riedinger, D.G. Sarantites and C.-H. Yu, *Phys. Rev. Lett.* 80 (1998) 3018.
- [15] F. Naulin, Jing-Ye Zhang, H. Flocard, D. Vautherin, P.-H. Heenen and P. Bonche, submitted to *Nucl. Phys. A*.
- [16] P.-H. Heenen, J. Terasaki, P. Bonche, H. Flocard and J. Skalski, *Czech. J. Phys.* (1998) in print, *Proc. Int. Conf. on Atomic Nuclei and Metallic Clusters: Finite Many-Fermion Systems*, Prague, Czech Republic, September 1997, ed. J. Kvasil
- [17] P.-H. Heenen, J. Terasaki, P. Bonche, H. Flocard, S.J. Krieger and M.S. Weiss, *Proc. XVII RCNP Int. Symp. on Innovative Computational Methods in Nuclear Many-Body Problems*, Osaka, Japan, November 1997 (World Scientific, Singapore).
- [18] G. Audi, O. Bersillon, J. Blachot and A.H. Wapstra, *Nucl. Phys. A* 624 (1997) 1.
- [19] D. Vautherin and D.M. Brink, *Phys. Rev. C* 3 (1972) 626.
- [20] M.J. Giannoni and Ph. Quentin, *Phys. Rev. C* 21 (1980) 2076.
- [21] E. Chabanat, Ph.D. Thesis, University of Lyon, France, 1995, unpublished.
- [22] P.-G. Reinhard and M. Girod, *Nucl. Phys. A* 389 (1982) 179.
- [23] P.-G. Reinhard and J. Friedrich, *Z. Phys. A* 321 (1985) 619; P.-G. Reinhard, private communication.
- [24] P.-G. Reinhard and C. Toepffer, *Int. J. Mod. Phys. E* 3 (1994) 435.
- [25] Y. Aboussir, J.M. Pearson, A.K. Dutta and F. Tondeur, *Nucl. Phys. A* 549 (1992) 155.
- [26] G. Audi and A.H. Wapstra, *Nucl. Phys. A* 595 (1995) 409.
- [27] J.-F. Berger, private communication.
- [28] C. Rigollet, Ph.D. Thesis, University of Strasbourg, France, 1996, unpublished.
- [29] N. Tajima, P. Bonche, H. Flocard, P.-H. Heenen and M.S. Weiss, *Nucl. Phys. A* 551 (1993) 434.
- [30] R.R. Chasman, *Phys. Rev. C* 14 (1976) 1935.
- [31] F. Tondeur, *Nucl. Phys. A* 315 (1979) 353.
- [32] G.F. Bertsch and H. Esbensen, *Ann. Phys. (N.-Y.)* 209 (1991) 327.
- [33] J. Terasaki, P.-H. Heenen, P. Bonche, J. Dobaczewski and H. Flocard, *Nucl. Phys. A* 593 (1995) 1.
- [34] P. Bonche, H. Flocard, P.-H. Heenen, S.J. Krieger and M.S. Weiss, *Nucl. Phys. A* 443 (1985) 39.
- [35] Z. Patyk and A. Sobieczewski, *Nucl. Phys. A* 626 (1997) 307c, *Proc. Third Int. Conf. on Nuclear Physics at Storage Rings*, STORI 96, Bernkastel-Kues, Germany, October 1996.
- [36] Nguyen Van Giai and V. Bernard, *Nucl. Phys. A* 348 (1980) 75.
- [37] N. Fukunishi, T. Otsuka and I. Tanihata, *Phys. Rev. C* 48 (1993) 1648.
- [38] K. Oyamatsu, I. Tanihata, Y. Sugahara, K. Sumiyoshi and H. Toki, *Nucl. Phys. A* (1998) to be published.
- [39] T. Suzuki, H. Geissel, O. Bochkarev, L. Chulkov, M. Golovkov, N. Fukunishi, D. Hirata, H. Irnich, Z. Janas, H. Keller, T. Kobayashi, G. Kraus, G. Münzenberg, S. Neumaier, F. Nickel, A. Ozawa, A. Piechaczek, E. Roeckl, W. Schwab, K. Sümmerner, K. Yoshida and I. Tanihata, *Phys. Rev. C* (1998) to be published.
- [40] M.M. Sharma, G.A. Lalazissis and P. Ring, *Phys. Lett. B* 317 (1993) 9; G.A. Lalazissis, M.M. Sharma, J. König and P. Ring, in *Nuclear Shapes and Nuclear Structure at Low Excitation Energies*, ed. M. Vergnes, D. Goutte, P.-H. Heenen and J. Sauvage (Editions Frontières, Paris, 1994) p. 161.
- [41] G.A. Lalazissis, M.M. Sharma, J. König and P. Ring, *Phys. Rev. Lett.* 74 (1995) 3744
- [42] J.-F. Berger, in *Nuclear Shapes and Nuclear Structure at Low Excitation Energies*, ed. M. Vergnes, D. Goutte, P.-H. Heenen and J. Sauvage (Editions Frontières, Paris, 1994) p. 1.
- [43] J. Terasaki, P.-H. Heenen, H. Flocard and P. Bonche, *Nucl. Phys. A* 600 (1996) 371.
- [44] R.D. Page, P.J. Woods, R.A. Cunningham, T. Davidson, N.J. Davis, S. Hofmann, A.N. James, K. Livingston, P.J. Sellin and A.C. Shotton, *Phys. Rev. Lett.* 68 (1992) 1287.
- [45] W. Nazarewicz, J. Dobaczewski and T.R. Werner, *Phys. Script. T* 56 (1995) 9.
- [46] J. Dobaczewski, W. Nazarewicz and T.R. Werner, *Phys. Script. T* 56 (1995) 15.
- [47] J. Dobaczewski, H. Flocard and J. Treiner, *Nucl. Phys. A* 422 (1984) 103.
- [48] M. Centelles, M. Del Estal, X. Viñas, *Nucl. Phys. A* (1998) to be published.
- [49] B. Grammaticos and A. Voros, *Ann. Phys. (N.-Y.)* 123 (1979) 359; 129 (1980) 153.
- [50] J.P. Blaizot and B. Grammaticos, *Nucl. Phys. A* 355 (1981) 115.
- [51] M. Brack, C. Guet and H.-B. Håkansson, *Phys. Rep.* 123 (1985) 275.
- [52] K. Kolehmainen, M. Prakash, J.M. Lattimer and J.R. Treiner, *Nucl. Phys. A* 439 (1985) 535.
- [53] C.J. Pethick and D.G. Ravenhall, *Ann. Rev. Nucl. Part. Sc.* 45 (1995) 429.

- [54] D. Von-Eiff, H. Freyer, W. Stocker and M.K. Weigel, Phys. Lett. B 344 (1985) 11.
- [55] G.A. Lalazissis, D. Vretenar, W. Pöschl and P. Ring, Nucl. Phys. A 632 (1998) 363.
- [56] G.A. Lalazissis, D. Vretenar, W. Pöschl and P. Ring, Phys. Lett. B 418 (1998) 7.
- [57] G.A. Lalazissis, D. Vretenar and P. Ring, Phys. Rev. C (1998) to be published.
- [58] D. Vretenar, G.A. Lalazissis and P. Ring, Phys. Rev. C (1998) to be published.
- [59] J. Dechargé and D. Gogny, Phys. Rev. C 21 (1980) 1568.
- [60] J.F. Berger, M. Girod and D. Gogny, Nucl. Phys. A 502 (1989) 85c.
- [61] M. Thies, Phys. Lett. B 166 (1986) 23.
- [62] P.-G. Reinhard, Rep. Prog. Phys. 52 (1989) 439.
- [63] R.J. Furnstahl and J.C. Hackworth, Phys. Rev. C 56 (1997) 2875.
- [64] R.J. Furnstahl, J.J. Rusnak and B.D. Serot, Nucl. Phys. A 632 (1998) 607.
- [65] M. Farine and J.M. Pearson, Phys. Rev. C 50 (1994) 185.
- [66] J. Dabrowski, Nukleonika 21 (1977) 143.
- [67] P.-G. Reinhard and H. Flocard, Nucl. Phys. A 584 (1995) 467.
- [68] B. Chen, J. Dobaczewski, K.-L. Kratz, K. Langanke, B. Pfeiffer, F.-K. Thielemann and P. Vogel, Phys. Lett. B 355 (1995) 37.
- [69] T.R. Werner, J.A. Sheikh, W. Nazarewicz, M.R. Strayer, A.S. Umar and M. Misu, Phys. Lett. B 333 (1994) 303.
- [70] G.A. Lalazissis, A.R. Farhan and M.M. Sharma, Nucl. Phys. A 628 (1998) 221.
- [71] J. Retamosa, E. Caurier, F. Nowacki and A. Poves, Phys. Rev. C 55 (1997) 1266.
- [72] O. Sorlin, D. Guillemaud-Mueller, A.C. Mueller, V. Borrel, S. Dogny, F. Pougheon, K.-L. Kratz, H. Gabelmann, B. Pfeiffer, A. Wöhr, W. Zeigert, Yu.E. Penionzhkevich, S.M. Lukyanov, V.S. Salamatin, R. Anne, C. Borcea, L.K. Fifield, M. Lewitowicz, M.G. Saint-Laurent, D. Bazin, C. Détraz, F.-K. Thielemann and W. Hillebrandt, Phys. Rev. C 47 (1993) 2941.
- [73] J.H. Kelley, T. Suomijärvi, S.E. Hirzebruch, A. Azhari, D. Bazin, Y. Blumenfeld, J.A. Brown, P.D. Cottle, S. Danczyk, M. Fauerbach, T. Glasmacher, J.K. Jewell, K.W. Kemper, F. Maréchal, D.J. Morrissey, S. Ottini, J.A. Scarpaci and P. Thirolf, Phys. Rev. C 56 (1997) R1206.
- [74] H. Scheit, T. Glasmacher, B.A. Brown, J.A. Brown, P.D. Cottle, P.G. Hansen, R. Harkewicz, M. Hellstöm, R.W. Ibbotson, J.K. Jewell, K.W. Kemper, D.J. Morrissey, M. Stiener, P. Thirolf and M. Thoennessen, Phys. Rev. Lett. 77 (1996) 3967.
- [75] M.M. Sharma, G.A. Lalazissis, W. Hillebrandt and P. Ring, Phys. Rev. Lett. 72 (1994) 1431.
- [76] P. Danielewicz and Q. Pan, Phys. Rev. C 46 (1992) 2002.
- [77] P. Danielewicz, Phys. Rev. C 51 (1995) 716.
- [78] R. Bougault, J.P. Wieleczko, M. D'Agostino, W.A. Friedman, F. Gulminelli, N. Leneindre, A. Chbihi, A. Le Fèvre, S. Salou, M. Assenard, G. Auger, C.O. Bacri, E. Bisquer, F. Bocage, B. Borderie, R. Brou, P. Buchet, J.L. Charvet, J. Colin, D. Cussol, R. Dayras, E. De Filippo, A. Demeyer, D. Doré, D. Durand, P. Eudes, J.D. Frankland, E. Galichet, E. Genouin-Duhamel, E. Gerlic, M. Germain, D. Gourio, D. Guinet, P. Laitesse, J.L. Laville, J.F. Lecolley, T. Lefort, R. Legrain, O. Lopez, M. Louvel, L. Nalpas, A.D. N'guyen, J. Péter, E. Plagnol, A. Rhamani, T. Reposeur, M.F. Rivet, M. Squalli, J.C. Steckmeyer, M. Stern, B. Tamain, L. Tassant-Got, O. Tirel, E. Vient and C. Volant, Proc. XXXV Int. Winter Meeting on Nuclear Physics, Bormio, Italy, February 1997, ed. I. Iori, Ricerca Scientifica ed Educazione Permanente, Suppl. 110, 1997.
- [79] E.W. Otten, in Treatise on Heavy-Ion Science, vol. 8, Nuclei far from Stability, ed. D.A. Bromley (Plenum, New York, 1989).

Update

Nuclear Physics, Section A

Volume 643, Issue 4, 7 December 1998, Page 441

DOI: [https://doi.org/10.1016/S0375-9474\(98\)00570-3](https://doi.org/10.1016/S0375-9474(98)00570-3)

Erratum

Erratum to “A Skyrme parametrization from subnuclear to neutron star densities. (II): Nuclei far from stabilities” [Nucl. Phys. A 635 (1998) 231–256] ^{*}

E. Chabanat ^a, P. Bonche ^b, P. Haensel ^c, J. Meyer ^{a,1}, R. Schaeffer ^b

^a *Institut de Physique Nucléaire de Lyon, CNRS-IN2P3 / Université Claude Bernard Lyon 1,
43, Bd. du 11.11.18, 69622 Villeurbanne Cedex, France*

^b *Service de Physique Théorique, CEA Saclay, 91191 Gif sur Yvette Cedex, France*

^c *N. Copernicus Astronomical Center, Polish Academy of Sciences, Bartycka 18, PL-00-716 Warsaw, Poland*

In Section 2, the nuclear central field $U_q(\mathbf{r})$ (Eq. (2.8)) and the spin-orbit field $W_q(\mathbf{r})$ (Eq. (2.9)) should read

$$\begin{aligned}
 U_q(\mathbf{r}) = & \frac{1}{2} t_0 [(2 + x_0) \rho - (1 + 2x_0) \rho_q] \\
 & + \frac{1}{24} t_3 \{ (2 + x_3) (2 + \alpha) \rho^{\alpha+1} - (2x_3 + 1) [2\rho^\alpha \rho_q + \alpha \rho^{\alpha-1} (\rho_p^2 + \rho_n^2)] \} \\
 & + \frac{1}{8} [t_1 (2 + x_1) + t_2 (2 + x_2)] \tau + \frac{1}{8} [t_2 (2x_2 + 1) - t_1 (2x_1 + 1)] \tau_q \\
 & + \frac{1}{16} [t_2 (2 + x_2) - 3t_1 (2 + x_1)] \nabla^2 \rho \\
 & + \frac{1}{16} [3t_1 (2x_1 + 1) + t_2 (2x_2 + 1)] \nabla^2 \rho_q \\
 & - \frac{1}{2} W_0 [\nabla \cdot \mathbf{J} + \nabla \cdot \mathbf{J}_q], \tag{2.8}
 \end{aligned}$$

$$W_q(\mathbf{r}) = \frac{1}{2} W_0 (\nabla \rho + \nabla \rho_q) + \frac{1}{8} (t_1 - t_2) \mathbf{J}_q - \frac{1}{8} (t_1 x_1 + t_2 x_2) \mathbf{J}. \tag{2.9}$$

^{*} PII of original article: S0375-9474(98)00180-8

¹ E-mail: jmeyer@ipnl.in2p3.fr